Available online at www.sciencedirect.com
ScienceDirect
Journal of the European Ceramic Society 29 (2009) 105–113
www.elsevier.com/locate/jeurceramsoc

Processing and properties of 0.65Pb($Mg_{1/3}Nb_{2/3}$)O_3–0.35$PbTiO_3$ thick films

Danjela Kuščer*, Miha Skalar, Janez Holc, Marija Kosec

Jozef Stefan Institute, Jamova 39, SI-1000 Ljubljana, Slovenia

Received 5 May 2008; accepted 17 June 2008
Available online 23 July 2008

Abstract

We have investigated the processing of 0.65Pb($Mg_{1/3}Nb_{2/3}$)O_3–0.35$PbTiO_3$ (PMN–PT) thick films on platinised alumina substrates. Nanosized PMN–PT powder with 2 mol% of excess PbO was prepared by high-energy milling and deposited on the substrate using screen-printing technology. The films were then sintered at 950 °C in a PbO-rich atmosphere. The influence of the sintering time and the amount of PbO-containing packing powder was studied and related to the structural, microstructural, dielectric and piezoelectric properties of the film. In order to obtain a homogeneous and dense thick film without any secondary phase, the PMN–PT films had to be sintered in the presence of a PbO-based liquid phase that had to be completely removed from the thick film during the final stage of the sintering. Under optimal sintering conditions we obtained a room temperature relative dielectric permittivity of 3600, dielectric losses of 0.036, a T_m of 174 °C, a permittivity at the T_m of 21,000 and a d_{33} of 140 pC/N.

Keywords: Films; Sintering; Microstructure-final; Dielectric properties; Perovskites

1. Introduction

Pb($Mg_{1/3}Nb_{2/3}$)O_3–$PbTiO_3$ (PMN–PT) ferroelectric materials have been widely investigated because of their outstanding piezoelectric properties. Since the properties are maximised for a composition close to the morphotropic phase boundary, i.e., PMN–PT with 35% of $PbTiO_3$, this composition is the most appropriate for producing actuators and sensors.[1,2] Thick-film technology offers many advantages over the use of bulk ceramics in various electronic devices. For example, conventional ceramic processing requires separate forming, machining and bonding of the components. In contrast, thick-film technology allows an active layer to be deposited directly onto the device component. This approach simplifies the manufacturing process considerably and reduces the costs. Screen-printing technology is extensively used for the processing of films with thicknesses ranging from a few micrometres to a few tens of micrometres on various substrates. In order to produce high-quality thick films, the starting PMN–PT powder should be chemically homogeneous and fine grained, the processing temperature should be as low as possible to minimise the chemical reactivity between the active layer and the substrate, the PMN–PT film needs to adhere to the substrate, and it should have a high density and the appropriate microstructural characteristics. The synthesis of perovskite PMN–PT is problematic because of the formation of a stable pyrochlore phase that has a negative effect on the dielectric properties of the perovskite phase. Various methods have been devised to eliminate this parasitic pyrochlore phase, such as the Columbite method,[3] the addition of excess MgO and/or PbO[4,5] and high-energy milling.[6,7]

The techniques for lowering the sintering temperature of lead-based ceramics rely on using fine, nanosized starting powder and/or adding compounds that ensure sintering in the presence of a liquid phase.[3,8] Researchers have used various compounds as a sintering aid, such as $Li_2B_4O_7$,[9] Cu_2O–PbO[10] and $LiBiO_2$–CuO.[11] The disadvantage of using these additives is that a second phase is introduced into the system, which can then reduce the functional properties of the bulk ceramic or the thick film.[12] Another approach is to use PbO as a sintering aid; as it is well known that the densification of a lead-based perovskite is considerably enhanced in the presence of PbO.[13–19] Due to the low melting point and the high vapour pressure of PbO, a liquid phase is formed that improves the densification process, but with careful control of the atmosphere during the processing

* Corresponding author. Tel.: +386 1477 3489; fax: +386 1477 3887.
E-mail address: danjela.kuscer@ijs.si (D. Kuščer).

0955-2219/$ – see front matter © 2008 Elsevier Ltd. All rights reserved.
doi:10.1016/j.jeurceramsoc.2008.06.010

the liquid phase can be removed from the active film.[13,14,20] It has also been reported that (Pb,La)(Zr,Ti)O_3 without any excess PbO starts to sinter at a temperature almost 300 °C higher than a sample with excess PbO.[16,21]

From the phase diagram of Pb($Mg_{1/3}Nb_{2/3}$)O_3–PbO it is evident that Pb($Mg_{1/3}Nb_{2/3}$)O_3 and PbO form a eutectic with the composition 74 wt.% PbO and 26 wt.% Pb($Mg_{1/3}Nb_{2/3}$)O_3 at a eutectic temperature of 830 °C.[22] No solubility of Pb($Mg_{1/3}Nb_{2/3}$)O_3 in PbO or vice versa is reported. Gorzkowski et al.[18] studied the influence of excess PbO on the growth mechanism of 0.65PMN–0.35PT and reported that the crystals only grow when a critical amount of PbO content is present at the grain boundaries of the PMN–PT. The critical amount of PbO is reached when there is sufficient to wet all the grain boundaries. Gorzkowski et al.[23] observed the existence of Mg, Nb and Ti in addition to Pb in the liquid phase at the grain boundaries at 1150 °C. They proposed that the grain growth of PMN–PT is a result of material diffusion from the shrinking grains to the growing grains in the liquid phase. For PMN–PT without PbO a much lower grain growth rate was reported.[18]

The crystal structure of PMN–PT is very complex, particularly in the compositional range close to the morphotropic phase boundary (MPB), and has been studied extensively. It was reported that with an increasing amount of $PbTiO_3$ the rhombohedral phase transforms to the monoclinic phase, and with a further increase in the amount of PT it transforms to the tetragonal phase.[24,25] In a systematic study of the $(1-x)$PMN–xPT compositions with $0.3 \le x \le 0.39$ by Noheda et al.[26] they showed that the rhombohedral phase exists for $x \le 0.31$ from 4 to 400 °C and the monoclinic phase exists in the compositional range $0.31 \le x \le 0.37$ for temperatures between 4 and 200 °C. At higher temperatures the monoclinic phase transforms into the tetragonal phase and the transition temperature depends on the chemical composition for temperatures higher than 200 °C. It was also shown that the composition 0.65PMN–0.35PT is tetragonal at room temperature. The evolution of the phases in the PMN–PT system at room temperature was reported by Kumar Singh and Pandey.[27] They showed that the structure of $(1-x)$PMN–xPT for $0.31 \le x \le 0.34$ is monoclinic, with the space group *Pm*; however, for $0.35 \le x \le 1$ it is tetragonal, with the space group *P*4*mm*.

The aim of our work was to study the processing of 0.65Pb($Mg_{1/3}Nb_{2/3}$)O_3–0.35$PbTiO_3$ thick-film structures on an alumina substrate using screen-printing technology. The sintering conditions of the PMN–PT thick films prepared from nanosized powder were studied in order to prepare a homogeneous and dense thick-film structure with a large functional response. The structural and functional properties of the PMN–PT thick films were correlated with the sintering conditions.

2. Experimental

For the experimental work we used PbO (99.9+%, Aldrich, Steinheim, Germany), MgO (98%, Aldrich, Steinheim, Germany), TiO_2 (99.8%, Alfa Aesar, Karlsruhe, Germany), Nb_2O_5 (99.9%, Aldrich, Steinheim, Germany) and ZrO_2 (99%, Tosoh, Japan).

A mixture of PbO, MgO, TiO_2 and Nb_2O_5 in the molar ratio corresponding to the stoichiometry 0.65Pb($Mg_{1/3}Nb_{2/3}$)O_3–0.35$PbTiO_3$ with 2 mol% of excess PbO (denoted PMN–PT) was high-energy milled in a planetary mill (Retsch, Model PM 400, Hann, Germany) for 64 h. A total of 200 g of powder was placed in the vial. The experimental details together with the properties of the powder are given in Refs. [6,28].

The PMN–PT was prepared from high-energy-milled powder pre-fired at 700 °C for 2 h. In order to improve the adhesion of the PMN–PT on the platinised alumina substrate, a Pb($Zr_{0.53}Ti_{0.47}$)O_3 layer (denoted PZT) was deposited between the electrode and the substrate.[29] The PZT was prepared by solid-state synthesis as described in Ref. [30]. The paste for the screen-printing was prepared from the PMN–PT and PZT powders combined with an organic vehicle. The alumina substrates were prepared by slip casting from Alcoa A-16 and sintered at 1700 °C for 4 h. The dimensions of the substrate were 28 mm × 28 mm and the thickness was 3 mm. The PZT paste was screen printed on the Al_2O_3 substrate and fired at 1100 °C for 2 h in a Pb-rich atmosphere. The platinum paste (Ferro 6412, Hanau, Germany) was screen printed on the PZT/Al_2O_3 substrate and fired at 1200 °C for 2 h. The PMN–PT paste was printed on the Pt/PZT/Al_2O_3 substrate and pre-fired at 500 °C for 1 h. The thick-film samples were sintered in a Pb-rich atmosphere. The sample was placed in a covered corundum vessel with a volume of 27 cm^3, and around the sample was placed the packing powder with the composition $PbZrO_3$ with 2 mol% excess of PbO. The samples were sintered at 950 °C for various times and various amounts of packing powder. The first set of samples was prepared with a fixed amount of packing powder (1 g) and various sintering times (2, 8 and 24 h). The second set of samples was sintered for a constant time of 2 h using various amounts of packing powder, i.e., 1, 1.5, 3 and 6 g.

The X-ray powder-diffraction data for the powders and thick films were collected at room temperature on a diffractometer (PANalytical, X′Pert PRO MPD, The Netherlands) using Cu Kα radiation. The data were collected in the 2θ range from 10° to 70°, in steps of 0.034°, with an integration time of 100 s. The phases were identified using the PDF-2[31] database.

A JEOL 5800 scanning electron microscope (SEM) equipped with a Tracor-Northern energy-dispersive system (EDS) was used for the overall microstructural analysis.

For the electrical measurements gold electrodes were sputtered onto the thick films. The real and the imaginary parts of the complex dielectric constant were measured with an HP 4284 A Precision LCR Meter. The dielectric permittivity versus temperature was measured in a furnace with a temperature uncertainty of ±2 °C. The samples were polarised at 2.5 kV/mm at 150 °C. The piezoelectric piezo d_{33} constant was measured using the Berlincourt method (Take control PM10).

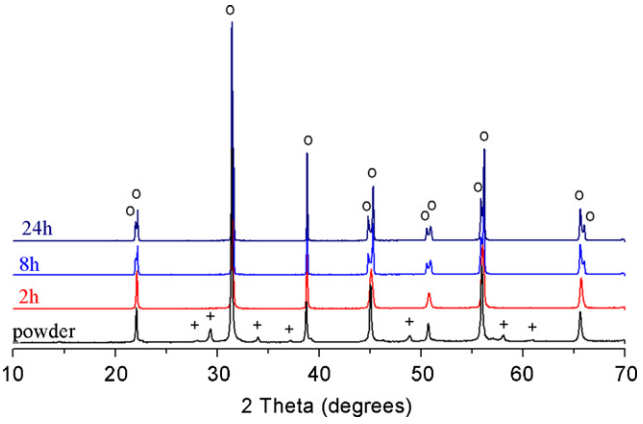

Fig. 1. X-ray powder-diffraction patterns of PMN–PT powder annealed at 700 °C and PMN–PT thick films sintered at 950 °C for 2, 8 and 24 h using 1 g of packing powder. (◯) $Pb(Mg_{1/3}Nb_{2/3})O_3$ and (+) pyrochlore.

3. Results and discussion

The X-ray powder-diffraction spectra of the mechanochemically synthesised PMN–PT powder annealed at 700 °C for 2 h together with PMN–PT thick films sintered at 950 °C for 2, 8 and 24 h using 1 g of packing powder are shown in Fig. 1. The powder annealed at 700 °C contained a perovskite phase together with a small amount of pyrochlore. In the thick-film structures annealed at 950 °C all the diffraction peaks corresponded to PMN–PT. We did not detect any extra diffraction peaks that might correspond to pyrochlore or PbO phases. We indexed all the PMN–PT structures with the nominal composition 0.65PMN–0.35PT using a tetragonal structure based on the literature data, which stated that $(1-x)$PMN–xPT with $x \geq 0.35$ crystallises in a tetragonal crystal structure at room temperature.[26,27] The calculated lattice parameters of the PMN–PT powder and the sintered thick films are shown in Table 1.

The XRD spectra of the PMN–PT powder and the PMN–PT film sintered for 2 h showed broad diffraction peaks with a pseudo-cubic character. The calculated lattice parameters of these two samples were similar. However, with a prolonged sintering time from 2 to 8 h the splitting of the diffraction peaks was evident, together with the decrease in the a spacing and the increase of the c spacing. It appeared that the lattice parameters of the PMN–PT thick film changed most significantly between 2 and 8 h of sintering. The lattice parameters of the 8- and 24-h sintered samples were similar and agreed well with the reported values for the bulk 0.65PMN–0.35PT composition having the tetragonal structure.[27]

Cross-sectional SEM images of the PMN–PT thick films on $Pt/PZT/Al_2O_3$ substrates with a chemically etched PMN–PT layer sintered at 950 °C for 2, 8 and 24 h using 1 g of packing powder are shown in Fig. 2a–f. The active layer showed good adhesion to the substrate as a result of using the PZT barrier layer between the Al_2O_3 and the electrode. All the sintered layers were porous and about 80 μm thick, and their thicknesses did not change significantly with the increasing sintering time (Table 1). The PMN–PT thick film sintered for 2 h consisted of agglomerated sub-micron-sized grains. We estimated that the grain size did not exceed 500 nm. However, with an increase of the sintering time the grain size increased: after 8 h of sintering the grain size was in the range of 1 μm, and this did not change significantly when the sintering time was prolonged to 24 h.

The second set of experiments was performed at a constant sintering temperature of 950 °C and a time of 2 h, but using various amounts of packing powder, i.e., 1, 1.5, 3 and 6 g. Cross-sectional SEM images of the PMN–PT thick films on $Pt/PZT/Al_2O_3$ substrates together with a chemically etched PMN–PT layer sintered with various amounts of packing powder are shown in Fig. 2a and b and in Fig. 3a–f. The thickness of the film decreased notably with the increasing amount of packing powder from 82 to 63 μm for 1 and 1.5 g of packing powder, respectively (Table 1). It is evident that when using a larger amount of packing powder the grain size increased from a few hundred nanometres to around 2 μm, indicating that grain-growth processes occurred. The microstructural analysis of the PMN–PT showed that the porosity of the samples decreased with the increasing amount of packing powder. The samples sintered with 1.5, 3 and 6 g of packing powder contained 22, 11 and 8% of pores, respectively, and the thickness decreased to 63, 55 and 45 μm, respectively. Simultaneously, the grain size of the PMN–PT increased, and reached 5 μm when sintered with 6 g of packing powder. A detailed analysis of the PMN–PT thick film sintered with 6 g of packing powder showed that the microstructure consisted of two phases. From the SEM image in Fig. 4 it is clear that the PMN–PT grains are surrounded with a bright phase. The EDS analysis showed that this bright phase contained primarily lead, and for that reason we assume that the phase was PbO-rich.

Table 1
Thickness, lattice parameters and c/a ratio of PMN–PT thick films sintered at 950 °C for various times and using various amounts of packing powder

T_{sint} (°C)	t_s (h)	m_{PP} (g)	d (μm)	a (nm)	c (nm)	c/a
700[a]				0.4017 ± 0.0001	0.4025 ± 0.0001	1.0020
950	2	1	82	0.40142 ± 0.00007	0.40260 ± 0.00009	1.0029
950	8	1	82	0.40033 ± 0.00005	0.40413 ± 0.00006	1.0095
950	24	1	80	0.40021 ± 0.00004	0.40420 ± 0.00005	1.0100
950	2	1.5	63	0.40023 ± 0.00003	0.40443 ± 0.00003	1.0104
950	2	3	55	0.40024 ± 0.00003	0.40445 ± 0.00004	1.0105
950	2	6	45	0.40026 ± 0.00005	0.40393 ± 0.00005	1.0092

Lattice parameters of PMN–PT powder annealed at 700 °C are also shown.
[a] Mechanochemically activated powder annealed at 700 °C for 2 h.

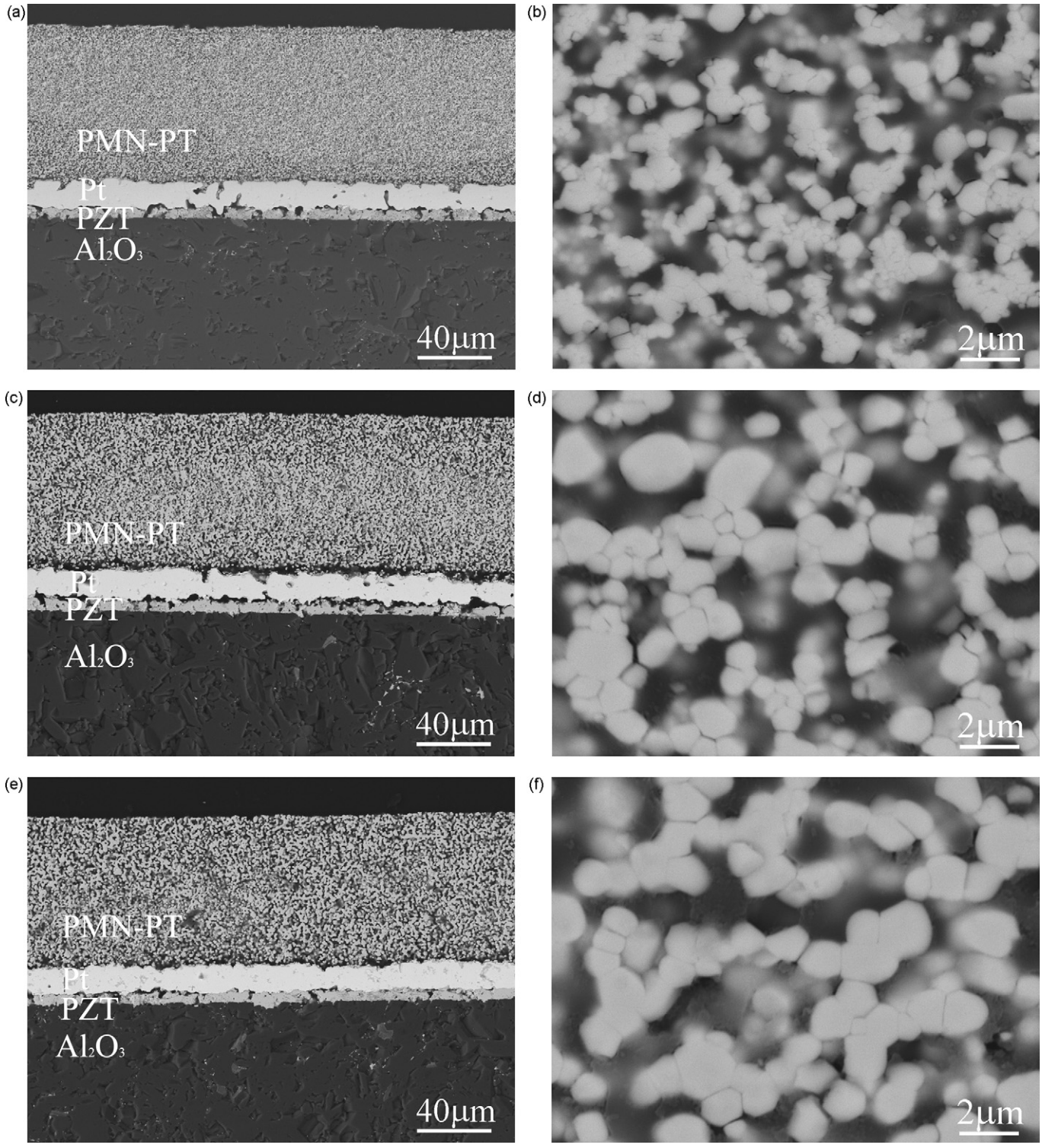

Fig. 2. SEM image of PMN–PT on a Pt/PZT/Al_2O_3 substrate and chemically etched PMN–PT layer fired at 950 °C, using 1 g of packing powder and sintering times (a, b) 2 h, (c, d) 8 h and (e, f) 24 h.

The XRD spectra of the samples sintered at 950 °C for 2 h using 1.5, 3 and 6 g of packing powder are shown in Fig. 5. The lattice parameters of the thick-film PMN–PT were calculated based on a tetragonal structure and are presented in Table 1. It is clear that they did not vary a great deal when the amount of packing powder exceeded 1.5 g. An XRD analysis showed that all the samples exhibited a single-phase perovskite structure with the exception of the sample sintered with 6 g of packing powder. One extra peak, with a low intensity, was observed at a 2θ of 28.5°. The inset in Fig. 5 shows that this diffraction peak corresponds to the 1 0 1 peak of PbO litharge (PDF 85–1739).[31] The existence of PbO in this sample clearly shows that when using 6 g of pack-

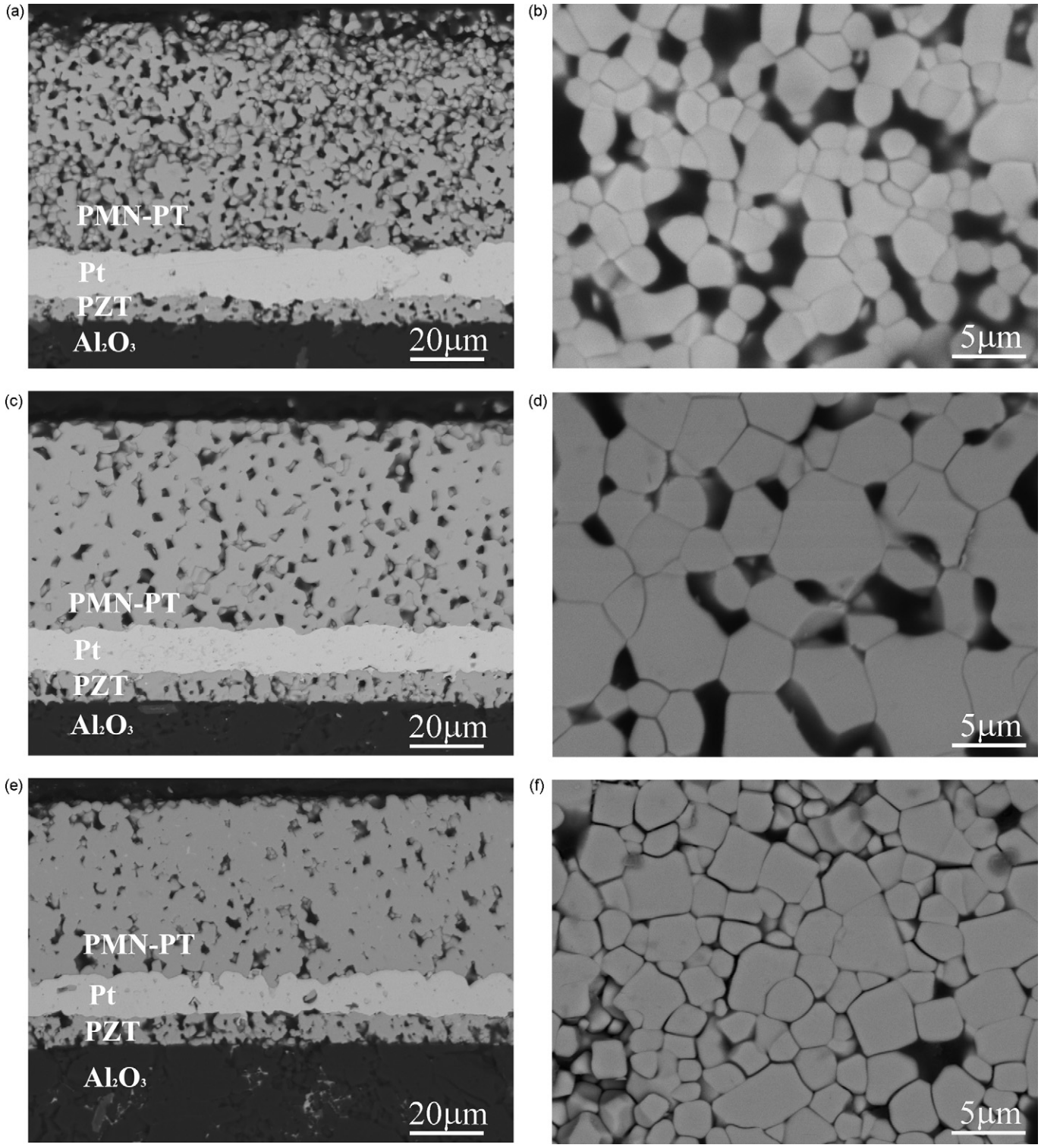

Fig. 3. SEM image of PMN–PT on Pt/PZT/Al_2O_3 substrate and chemically etched PMN–PT layer fired at 950 °C for 2 h using (a, b) 1.5 g, (c, d) 3 g and (e, f) 6 g of packing powder.

ing powder the PbO remained in the PMN–PT during the whole course of the sintering. As a result, the PMN–PT was sintered in the presence of a liquid phase and a dense microstructure was produced.

The dielectric permittivities and the piezoelectric d_{33} constants of the PMN–PT sintered at 950 °C for 2, 8 and 24 h with 1 g of packing powder are shown in Fig. 6 and in Table 2. All the samples showed broad and frequency-dependent ferroelectric-to-paraelectric transitions typical for relaxor ferroelectrics. The dielectric permittivity of the samples sintered for 2 h with 1 g of packing powder showed the broadest maximum of all the samples, with a peak value of 6 0 0. The sharpening of

Table 2
Dielectric, ferroelectric and piezoelectric properties of PMN–PT thick films sintered at 950 °C for various times and with various amounts of packing powder

t_{sint} (h)	m_{PP} (g)	ε (1 kHz at T_{room})	$tg\ \delta$ (1 kHz)	T_m (°C, 1 kHz)	ε (1 kHz at T_m)	d_{33} (pC/N)
2	1	260	0.035	174	600	57
8	1	345	0.036	172	1,300	55
24	1	350	0.023	170	1,370	54
2	1.5	2200	0.03	172	17,400	90
2	3	3600	0.036	174	21,000	140
2	6	2020	0.033	174	4,840	125

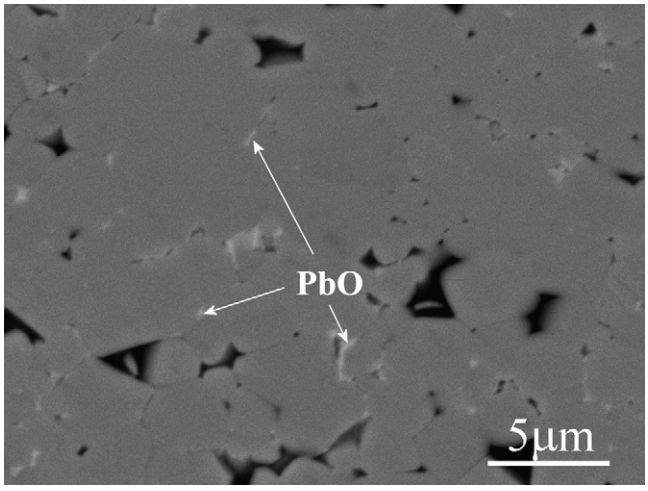

Fig. 4. SEM image of PMN–PT on Pt/PZT/Al_2O_3 substrate fired at 950 °C for 2 h using 6 g of packing powder. PbO-rich liquid phase is denoted as PbO.

the permittivity-versus-temperature curves together with the increase in the peak value of the permittivity was observed for increasing sintering times. The dielectric permittivity of the samples sintered for 8 h was 1300 at T_m, and this increased only slightly, i.e., to 1370 at T_m, after a prolonged sintering time of 24 h. We observed that the temperature of the transition to the paraelectric state, T_m, did not change a great deal with the increasing sintering time and is consistent with the literature data.[32] In addition, our results indicated that the piezoelectric d_{33} constant did not change significantly with a longer sintering time.

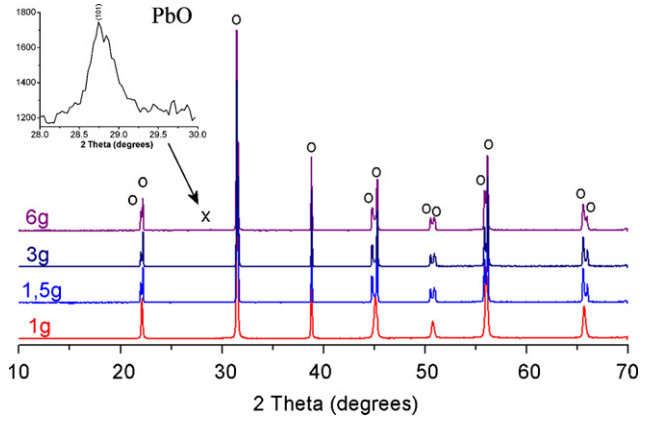

Fig. 5. X-ray powder-diffraction patterns of PMN–PT thick films sintered at 950 °C for 2 h using 1, 1.5, 3 and 6 g of packing powder. (◯) $Pb(Mg_{1/3}Nb_{2/3})O_3$ and (×) PbO.

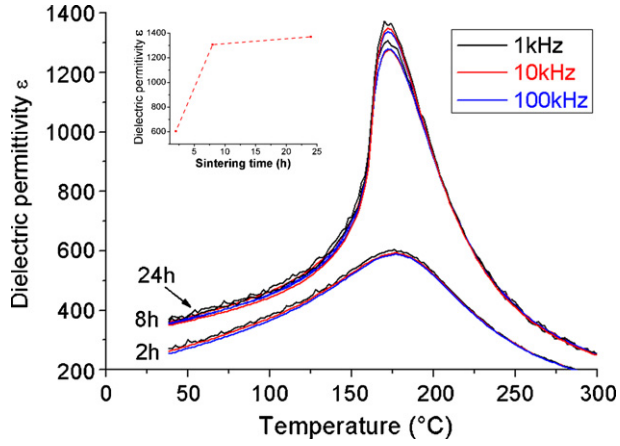

Fig. 6. The real part of the dielectric permittivity of PMN–PT thick films sintered at 950 °C for 2, 8 and 24 h using 1 g of packing powder as a function of temperature. (For interpretation of the references to color in this figure legend, the reader is referred to the web version of the article.)

The dielectric permittivity and the piezoelectric d_{33} constant of the PMN–PT films sintered at 950 °C for 2 h using 1, 1.5, 3 and 6 g of packing powder as a function of temperature are shown in Fig. 7 and in Table 2. It is clear that there was an enormous increase in the dielectric permittivity at room temperature as well as at T_m for the PMN–PT layers sintered with 1, 1.5 or 3 g of packing powder. The dielectric permittivity increased from 600 to 17,400 and 21,000 when increasing the amount of

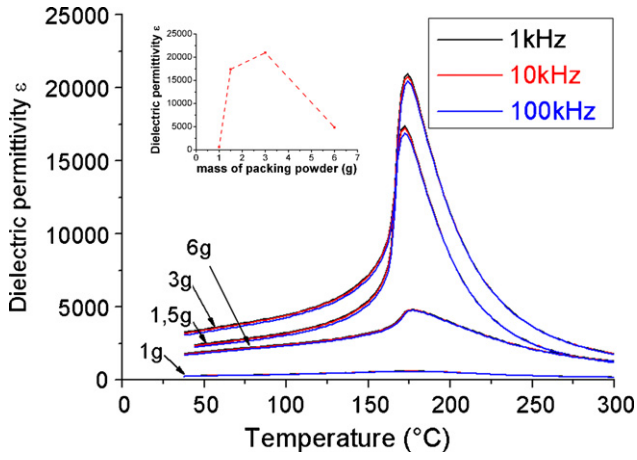

Fig. 7. The real part of the dielectric permittivity of PMN–PT thick films sintered at 950 °C for 2 h using 1, 1.5, 3 and 6 g of packing powder as a function of temperature. (For interpretation of the references to color in this figure legend, the reader is referred to the web version of the article.)

packing powder from 1 to 1.5 and 3 g. A sharpening of the ε–T curve is also clearly evident. The samples sintered with 1.5 and 3 g of packing powder exhibited a sharp ε–T behaviour and a weak T_m frequency dependence. From the result it is clear that the transition temperature T_m was constant, within the experimental uncertainty, and did not depend on the amount of packing powder (Table 2). We observed that the dielectric permittivity at T_m and d_{33} increased with an increasing amount of packing powder up to 3 g; however, with a further increase they decreased significantly. The dielectric permittivity and the d_{33} piezoelectric coefficient of the sample sintered with 6 g of packing powder was significantly lower, i.e., 4840 and 125 pC/N, compared to the samples sintered with 3 g of packing powder, i.e., 21,000 and 140 pC/N (Table 1). We assume that the reduction in the properties for the samples sintered with 6 g of packing powder can be attributed to the PbO, which was observed in the PMN–PT using XRD (Fig. 5) and at its phase boundaries using SEM (Fig. 4). It is well known that the PbO liquid phase improves the densification process of lead-based materials; however, when present at the grain boundaries it degrades the electrical properties of the perovskite phase noticeably.[14,33,38]

In order to prepare PMN–PT thick films with the desired functional response, the material has to be dense but without any secondary phase. To improve the densification of PMN–PT thick films, the presence of a liquid phase during the sintering is necessary. This can be done by adding an excess of PbO to the PMN–PT. Additionally, in order to prevent the sublimation of PbO from the layer during the sintering, the packing powder containing PbO was applied. As a result of the high vapour pressure of PbO at 950 °C, the PbO tended to sublimate from both the thick film and from the packing powder. Since the crucible where the sample was placed is a semi-closed system, it was possible that the PbO might sublimate out of this system. In order to ensure the liquid-phase sintering of the PMN–PT thick films, it is necessary for a certain amount of PbO to remain in the thick film. This can be done by adding packing powder around the sample. Two cases have to be considered. First, when the sample was surrounded by a small amount of packing powder, in our case 1 g, all the excess PbO sublimated from the PMN–PT in the initial stage of sintering. Since the system is semi-closed, the PbO from the packing powder sublimated out of the system. As a consequence, the excess PbO from the PMN–PT also sublimated and after a certain sintering time the PMN–PT did not contain any more excess PbO. This meant that the period when the liquid PbO was present in the PMN–PT was not sufficiently long to obtain a dense PMN–PT layer. It is clear that with a prolonged sintering time from 2 to 24 h the thickness of the PMN–PT layer did not change. This indicates that the densification process did not speed up significantly with time (Table 1). As a result, poor functional properties were obtained for the PMN–PT thick film sintered at 950 °C with 1 g of packing powder. We suppose that for 1 g of packing powder all the excess PbO added to the PMN–PT sublimated in the initial stage of the sintering and after this time the sintering of the PMN–PT occurred in the solid-state.

The second case looked at the condition when a larger amount of packing powder was used during the sintering of the PMN–PT. It appears that when using more than 1.5 g of packing powder around the sample, the excess PbO remained in the PMN–PT for a longer period of the thermal treatment. It is evident that the thickness and the porosity of the film decreased with the increasing amount of packing powder. We assume that in the PMN–PT layer surrounded with a larger amount of packing powder the liquid PbO was present for a longer time compared to the experiment with 1 g of packing powder. This hypothesis is supported by indirect evidence obtained from a microstructural analysis. With the largest amount of packing powder the PbO was present in the sample during the whole course of the sintering. The PMN–PT film was the thinnest, the least porous and PbO was still detected at the grain boundaries. When using 1.5 and 3 g of packing powder the film was thicker and the dielectric permittivity increased significantly as a result of PbO-free grain boundaries and a relatively dense microstructure.

In order to explain the relation between the structural and microstructural characteristics, and the functional response of the PMN–PT thick films, it is important to understand the structure of the PMN–PT at the atomic level. The relaxor ferroelectric properties originate from the frustration of the local polarisation due to the composition and the field inhomogeneities, which prevent long-range ferroelectric order. The dielectric properties of PMN-based materials depend directly on the degree of ordering of the magnesium and niobium cations in the perovskite cell, i.e., the B-site ordering. Our starting PMN–PT powder was prepared by mechanochemical synthesis.[6] The advantage of this method is the formation of a nanosized powder together with good chemical homogeneity in the nanoscale region.[34] The powder is chemically homogeneous on the micrometer level; however, such a powder seems to be highly B-site disordered at the atomic level. Gao et al.[35] reported that the mechanical activation induces B-site disordering in $Pb(Mg_{1/3}Nb_{2/3})O_3$–$Pb(Mg_{1/2}W_{1/2})O_3$. It was also shown that the addition of $PbTiO_3$ to $Pb(Mg_{1/3}Nb_{2/3})O_3$ decreases the B-site order.[36,37] Papet et al.[38] showed that the characteristics of the relaxor were related not only to the B-site order but also to the particle size and to the processing conditions. Significantly higher values of dielectric permittivity were observed for 6.2-μm- than for 300-nm-sized PMN particles. Similar observations were reported by Alguero et al.[39] This group observed that 4-μm-sized 0.65PMN–0.35PT particles consist of lamellar, wedge and crosshatched domains; however, 150-nm-sized particles contain only crosshatched domains. They also reported a sharper ε–T response and a higher dielectric permittivity for the sample with 4-μm grains than for the sample with 150-nm grains.

We believe that in the PMN–PT layer sintered at 900 °C for 2 h the degree of disorder at the atomic level is considerable and that the sample contained small domains. The grain size in this sample is well below 1 μm, and the pseudo-cubic character of this sample and the low permittivity at T_m support this hypothesis and agree well with the literature data.[39,40]

With prolonged sintering times to 8 and 24 h, the pseudo-cubic character of the PMN–PT vanished, and the grain size and the dielectric permittivity increased. We believe that the degree of ordering in the PMN–PT also increases. This increase

in the ordering in the PMN favours ferroelectric behaviour, i.e., a less diffuse phase transition and a reduction of the frequency dispersion.[36] Zhang and Wang[41] reported that the order–disorder transition is sluggish and occurs via atomic diffusion. It can be induced by annealing at high temperatures, and it was shown that an order–disorder transition occurs at 600 °C for $Pb(Mg_{1/3}Nb_{2/3})O_3$–$Pb(Mg_{1/2}W_{1/2})O_3$, at less than 900 °C for $Pb(Mg_{1/3}Nb_{2/3})O_3$ and for terbium-doped PMN at 1250 °C after 24 h.[35,37,42] The dielectric permittivity of the PMN–PT thick films sintered for 8 and 24 h is low and we believe that one possible reason for this is the lack of density. When sintering PMN–PT for 8 or 24 h using 1 g of packing powder, all the excess PbO sublimated from the thick film. In order to obtain a dense PMN–PT layer, the presence of liquid-phase PbO in the PMN–PT is necessary during the sintering process.[17,23]

The PMN–PT thick films sintered with a larger amount of packing powder showed a larger grain size and a lower porosity, indicating that grain growth and densification occurred. The microstructural characteristics were reflected in a significantly higher dielectric permittivity at room temperature and at T_m. The observed changes in the dielectric behaviour of the PMN–PT thick films cannot be attributed only to microstructural properties, these changes are also related to properties on the nanometre scale, such as domain type and size.

The results of this work suggest that the functional properties of PMN–PT thick films depend a great deal on the parameters used during the processing of the PMN–PT thick film. The homogeneous, nanosized starting PMN–PT powder is necessary to ensure sintering at a temperature as low as possible in order to prevent any chemical interaction between the active layer and the substrate. The sintering in the presence of the liquid phase within the whole course of the sintering process is necessary to obtain a dense microstructure with micron-sized grains. In addition, it is essential that the sintered PMN–PT thick film does not contain any PbO liquid phase. This must be completely removed from the grain boundaries during the final stage of the sintering process.

4. Summary

Thick-film $0.65Pb(Mg_{1/3}Nb_{2/3})O_3$–$0.35PbTiO_3$ structures on platinised alumina substrates were prepared from high-energy-milled nanosized powder using screen-printing technology. All the films exhibited good adhesion to the Pt/PZT/Al_2O_3 substrate.

The high-energy-milled powder makes possible the processing of chemically homogeneous PMN–PT thick films at 950 °C. The excess of PbO in the PMN–PT together with the optimal amount of packing powder enabled the sintering of PMN–PT in the presence of a liquid phase, resulting in a dense thick film with good properties. The optimal functional response was obtained for a PMN–PT thick film sintered at 950 °C for 2 h with 3 g of packing powder. We achieved a room temperature relative dielectric permittivity of 3600, dielectric losses of 0.036, a T_m of 174 °C, a permittivity at T_m of 21,000 and a d_{33} of 140 pC/N.

Acknowledgements

The Slovenian Research Agency and the European Community, through its MINUET project within the 6FP, are acknowledged for their financial support. Mrs. Jena Cilenšek and Mr. Silvo Drnovšek are thanked for their technical assistance.

References

1. Park, S. E. and Shrout, T. R., Ultrahigh strain and piezoelectric behaviour in relaxor based ferroelectric single crystals. *J. Appl. Phys.*, 1997, **82**, 1804–1811.
2. Haertling, G. H., Ferroelectric ceramics: history and technology. *J. Am. Ceram. Soc.*, 1999, **82**(4), 797–818.
3. Swartz, S. L. and Shrout, T. R., Fabrication of perovskite lead magnesium niobate. *Mat. Res. Bull.*, 1982, **17**, 1245–1250.
4. Guha, J. P., Hong, D. J. and Anderson, H., Effect of excess PbO on the sintering characteristics and dielectric properties of $Pb(Mg_{1/3}Nb_{2/3})O_3$–$PbTiO_3$ based ceramics. *J. Am. Ceram. Soc.*, 1988, **71**(3), C-152–C-154.
5. Kusumoto, K. and Sekiyo, T., Processing and propoerties of $(1-x)$ $Pb(Mg_{1/3}Nb_{2/3})O_3$–$xPbTiO_3$ solid solution from PbO- and MgO-excess composition. *Mat. Res. Bull.*, 1998, **33**(9), 1367–1375.
6. Kuscer, D., Holc, J. and Kosec, M., $0.65Pb(Mg_{1/3}Nb_{2/3})O_3$–$0.35$ $PbTiO_3$ formation by high-energy milling process. *J. Am. Ceram. Soc.*, 2007, **90**(1), 29–35.
7. Baek, J., Isobe, T. and Senna, M., Synthesis of pyrochlore free $0.9Pb(Mg_{1/3}Nb_{2/3})O_3$–$0.1$ $PbTiO_3$ ceramics via a soft mechanochemical route. *J. Am. Ceram. Soc.*, 1997, **80**(4), 973–981.
8. Kwon, S., Sabolsky, E. and Messing, G. L., Low-temperature reactive sintering of 0.65PMN–0.35PT. *J. Am. Ceram. Soc.*, 2001, **84**, 648–650.
9. Gentil, S., Damjanovic, D. and Setter, N., Develpoment of relaxor ferroelectric materials for screen-printing on alumina and silicon substrates. *J. Eur. Ceram. Soc.*, 2005, **25**, 2125–2128.
10. Dorey, R. A. and Whatmore, R. W., Electrical properties of high density PZT and PMN–PT/PZT thick films produced using ComFi technology. *J. Eur. Ceram. Soc.*, 2004, **24**, 1091–1094.
11. Wang, X. X., Murakami, K., Sugiyama, O. and Kaneko, S., Piezoelectric properties, densification behaviour and microstructural evaluation of low-temperature sintered PZT ceramics with sintering aids. *J. Eur. Ceram. Soc.*, 2001, **21**, 1367–1370.
12. Dorey, R. A. and Whatmore, R. W., Electroceramic thick film fabrication for MEMS. *J. Electroceram.*, 2004, **12**, 19–32.
13. Snow, G. S., Fabrication of transparent electrooptic PLZT ceramic by atmosphere sintering. *J. Am. Ceram. Soc.*, 1973, **56**(2), 91–96.
14. Kosec, M., Holc, J., Malič, B. and Bobnar, V., Processing of high performance lead lanthanum zirconate titanate thick films. *J. Eur. Ceram. Soc.*, 1999, **19**, 949–954.
15. Saha, D., Sen, A. and Maiti, H. S., Low temperature liquid phase sintering of lead magnesium niobate. *Ceram. Int.*, 1999, **25**, 145–151.
16. Kosec, M., Murko, D., Holc, J., Malič, B., Čeh, M., Hauke, T. *et al.*, Low-temperature processing of $(Pb,La)(Zr,Ti)O_3$ thick films on alumina substrates. *Z. Met. Kd.*, 2001, **92**(2), 97–104.
17. Guha, J. P., Hong, D. J. and Anderson, H. U., Effect of excess PbO on the sintering characteristic and dielectric properties of $Pb(Mg_{1/3}Nb_{2/3})O_3$–$PbTiO_3$-based ceramics. *J. Am. Ceram. Soc.*, 1998, **71**, C152–154.
18. Gorzkowski, E. P., Chan, H. M. and Harmer, M. P., Effect of PbO on the kinetics of $\{0\,0\,1\}Pb(Mg_{1/3}Nb_{2/3})O_3$–35 mol% $PbTiO_3$ single crystal grown into fully dense matrices. *J. Am. Ceram. Soc.*, 2006, **89**(3), 856–862.
19. Kosec, M., Holc, J., Kuscer, D. and Drnovsek, S., $Pb(Mg_{1/3}Nb_{2/3})O_3$–$PbTiO_3$ thick films from mechanochemically synthesised powder. *J. Eur. Ceram. Soc.*, 2007, **27**, 3775–3778.
20. Northrop, D. A., Vaporization of lead zirconate–lead titanate materials. *J. Am. Ceram. Soc.*, 1967, **50**(9), 441–445.

21. Kuščer, D., Korzekwa, J., Kosec, M. and Skulski, R., A- and B-compensated PLZT *x*/90/10: sintering and microstructural analysis. *J. Eur. Ceram. Soc.*, 2007, **27/16**, 4499–4507.
22. Ye, Z. G., Tissot, P. and Schmid, H., Pseudo-binary $Pb(Mg_{1/3}Nb_{2/3})O_3$–PbO phase diagram and crystal growth of $Pb(Mg_{1/3}Nb_{2/3})O_3$ (PMN). *Mater. Res. Bull.*, 1990, **25**, 739–748.
23. Gorzkowski, E. P., Watanabe, M., Chan, H. M. and Harmer, M. P., Effect of liquid phase chemistry on single-crystal growth in PMN–PT. *J. Am. Ceram. Soc.*, 2006, **89**(7), 2249–2286.
24. Kiat, J. M., Uesu, Y., Dkhil, B., Matsuda, M., Malibert, C. and Calvarin, G., Monoclinic structure of undoped morphotropic high piezoelectric PMN–PT and PZN–PT. *Phys. Rev. B*, 2002, **65**, 064106.
25. Xu, G., Luo, H., Xu, H. and Yin, Z., Third ferroelectric phase in PMNT single crystals near the morphotropic phase boundary composition. *Phys. Rev. B*, 2001, **64**, 020102.
26. Noheda, B., Cox, D. E. and Shirane, G., Phase diagram of the ferroelectric relaxor $(1-x)Pb(Mg_{1/3}Nb_{2/3})O_3$–$xPbTiO_3$. *Phys. Rev. B*, 2002, **66**, 054104.
27. Kumar Singh, A. and Pandey, D., Evidence for Mb and Mc phases in the morphortopic phase boundary region of $(1-x)$ $Pb(Mg_{1/3}Nb_{2/3})O_3$–$xPbTiO_3$: a Rietveld study. *Phys. Rev. B*, 2003, **67**, 064102-1–064102-12.
28. Kuscer, D., Meden, A., Holc, J. and Kosec, M., The mechano-synthesis of lead–magnesium–niobate ceramics. *J. Am. Ceram. Soc.*, 2006, **89**, 3081–3088.
29. Uršič, H., Škarabot, M., Hrovat, M., Holc, J., Skalar, M., Bobnar, V. *et al.*, The electrostrictive effect in ferroelectric $0.65Pb(Mg_{1/3}Nb_{2/3})O_3$-$0.35PbTiO_3$ thick films. *J. Appl. Phys.*, 2008, **103**(12), 124101, 1-4.
30. Tran-Huu-Hue, P., Levassort, F., Meulen, F. V., Holc, J., Kosec, M. and Lethiecq, M., Preparation and electromechanical properties of PZT/PGO thick films on alumina substrate. *J. Eur. Ceram. Soc.*, 2001, **21**(10–11), 1445–1449.
31. PDF-ICDD, PCPDFWin Version 2.2, June 2001. International Centre for Diffraction Data; 2002.
32. Leite, E. R., Scotch, A. M., Khan, A., Li, T., Chan, H. M. and Harmer, M. P., Chemical heterogeneity in PMN–0.35PT ceramics and effects on dielectric and piezoelectric properties. *J. Am. Ceram. Soc.*, 2002, **85**(12), 3018–3024.
33. Swartz, S. L., Shrout, T. R., Sulze, W. A. and Cross, L. E., Dielectric properties of lead–magnesium–niobate ceramics. *J. Am. Ceram. Soc.*, 1984, **67**(5), 311–315.
34. Suryanarayana, C., Mechanical alloying and milling. *Progress Mater. Sci.*, 2001, **46**, 1–184.
35. Gao, X., Xue, J., Yu, T., Shen, Z. and Wang, J., B-site order–disorder in $Pb(Mg_{1/3}Nb_{2/3})O_3$–$Pb(Mg_{1/2}W_{1/2})O_3$ triggered by mechanical activation. *J. Am. Ceram. Soc.*, 2002, **85**, 833–838.
36. Hilton, A. D., Barber, D. J., Randal, C. A. and Shrout, T. R., On short range ordering in the perovskite lead magnesium niobate. *J. Mater. Sci.*, 1990, **25**, 3461–3466.
37. Davies, P. K. and Akbas, M. A., Chemical order in PMN-related relaxors: structure, stability, modification, and impact on properties. *J. Phys. Chem. Solids*, 2000, **61**, 158–166.
38. Papet, P., Doughterty, J. P. and Shrout, T. R., Particle and grain size effects on the dielectric behaviour of the relaxor ferreoelectric $Pb(Mg_{1/3}Nb_{2/3})O_3$. *J. Mater. Res.*, 1990, **5**(12), 2902–2909.
39. Alguero, M., Ricorte, Jimenez, R., Ramos, P., Carreaud, J., Dkhil, B. *et al.*, Size effect in morphotropic phase boundary $Pb(Mg_{1/3}Nb_{2/3})O_3$–$PbTiO_3$. *Appl. Phys. Lett.*, 2007, **91**, 112905.
40. Bai, F., Li, J. and Viehland, D., Domain engineering states over various length scales in (0 0 1)-oriented $Pb(Mg_{1/3}Nb_{2/3})O_3$–*x*% $PbTiO_3$ crystals: electrical history dependence of hierarchal domains. *J. Appl. Phys.*, 2005, **97**, 054103.
41. Zhang, X. W. and Wang, Q., Study of the order-disorder transition in $A(B'B'')O_3$ perovskite type ceramics. *J. Am. Ceram. Soc.*, 1991, **74**(11), 2846–2850.
42. Akbas, M. A. and Davies, P. K., Thermally induced coarsening of the chemically ordered domains in $Pb(Mg_{1/3}Nb_{2/3})O_3$ (PMN)-based relaxors. *J. Am. Ceram. Soc.*, 2000, **83**(1), 119–123.